ELSEVIER

Journal of Volcanology and Geothermal Research 98 (2000) 117–126

Journal of volcanology and geothermal research

www.elsevier.nl/locate/jvolgeores

The relationship between degassing and ground deformation at Soufriere Hills Volcano, Montserrat

I.M. Watson[a,*], C. Oppenheimer[a], B. Voight[c], P.W. Francis[b], A. Clarke[c], J. Stix[d], A. Miller[e], D.M. Pyle[f], M.R. Burton[a,b], S.R. Young[g], G. Norton[g], S. Loughlin[g], B. Darroux[h], MVO Staff[h]

[a]*Department of Geography, University of Cambridge, Downing Place, Cambridge CB2 3EN, UK*
[b]*Department of Earth Sciences, Open University, Milton Keynes, Bucks, UK*
[c]*Department of Geosciences, Penn State University, PA, USA*
[d]*Département de Géologie, Université of Montréal, Montréal, Canada*
[e]*Geowalks, 24 Argyle Place, Edinburgh, UK*
[f]*Department of Earth Sciences, University of Cambridge, Cambridge, UK*
[g]*British Geological Survey, West Mains Road, Edinburgh, UK*
[h]*Montserrat Volcano Observatory, Mongo Hill, Montserrat, WI, USA*

Received 18 November 1999

Abstract

We examine the correlations between SO_2 emission rate, seismicity and ground deformation in the month prior to the 25 June 1997 dome collapse of the Soufriere Hills Volcano, Montserrat. During this period, the volcano exhibited a pattern of cyclic inflation and deflation with an 8–14 h period. We find that SO_2 emission rates, measured by COSPEC, correlate with the amplitude of these tilt cycles, and that higher rates of SO_2 emission were associated with stronger ground deformation and enhanced hybrid seismicity. Within tilt cycles, degassing peaks coincide with maximum deformation gradients. Increases in the amount of gas in the magma conduit feeding the dome, probably due to increases in volatile content of ascending magma volume can account for the observed increases in tilt amplitude, hybrid seismicity and SO_2 emission rate.

Keywords: degassing–deformation correlation; cyclic activity; COSPEC; Soufriere Hills Volcano

1. Introduction

Soufriere Hills Volcano (SHV), Montserrat, began erupting on 18 July 1995 with phreatic explosions, following seismic crises in 1992 and 1994 (Young et al., 1997). A new andesitic lava dome was first observed on 15 November 1995. Subsequent development of the eruption included periods of rapid dome growth, explosive events, and gravitational dome and fountain collapse generating pyroclastic density currents (Young et al., 1998a). At the time of writing (July 1999), there has been no dome growth since March 1998, though SO_2 emission rates remain at elevated levels of around 2–3 kg s^{-1}. Surveillance at SHV has been carried out by the Montserrat Volcano Observatory (MVO), comprised of local and visiting scientists, and using a combination of seismology, ground deformation, petrology and geochemistry,

* Corresponding author.

0377-0273/00/$ - see front matter
PII: S0377-0273(99)00187-0

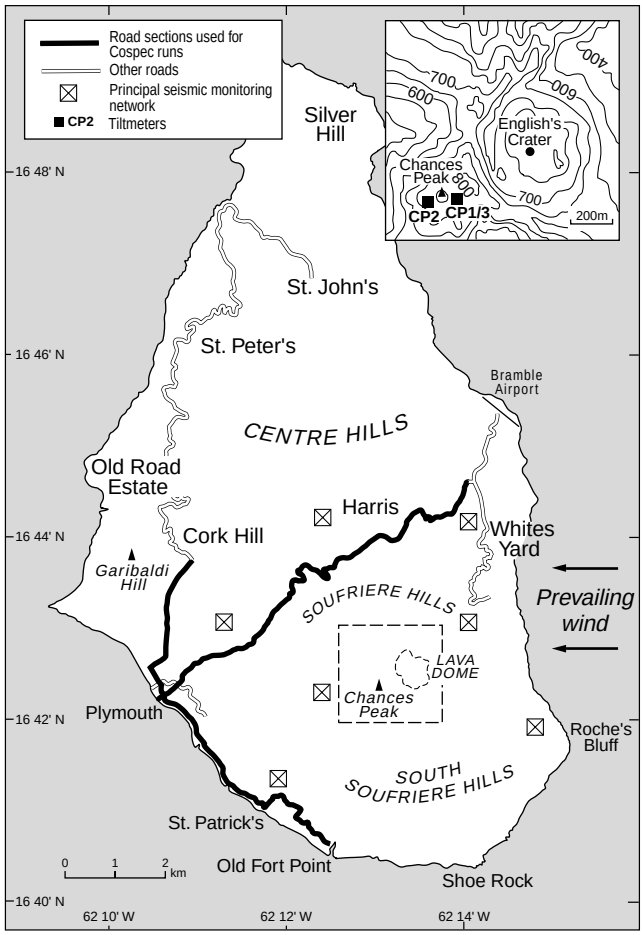

Fig. 1. Map of SHV showing principal seismic monitoring network and the roads used for the COSPEC measurement runs. Inset shows orientation of tiltmeters on Chances Peak. X-axis azimuths for the three tiltmeters are CP1, 054; CP2, 002; and CP3, 099. Subtract 90 for y axes (after Voight et al., 1999).

dome mapping, gas chemistry and environmental ash and ground water monitoring (Young et al., 1997, 1998a).

During late May and June 1997, SHV exhibited remarkably cyclic ground deformation (Voight et al., 1998, 1999) and correlated seismicity (Miller et al., 1998) with a mean period of 8–14 h. A typical tilt cycle consisted of inflation accompanied by a hybrid earthquake swarm which intensified as the inflation peaked, and often graded into tremor (Miller et al., 1998). Deflation coincided with the end of the hybrid activity and was associated with rockfalls and occasionally pyroclastic activity. These cycles preceded one of the largest collapse events during the whole eruption that took place on 25 June 1997. The aim of this paper is to compare the degassing record for the volcano at this time, available from correlation spectrometer (COSPEC) measurements, with deformation and seismic data. This is important because the dynamics of degassing are critical to understanding pressure fluctuations in the magmatic system and consequent switches in eruption style.

2. SO_2 degassing associated with dome-building eruptions

COSPEC datasets exist for a number of dome-building

Table 1
Details of COSPEC SO_2 emission rate data

Date	Time	Emission rate (kg/s)	Daily mean (kg/s)
24/05/97	14:30	11.61	11.13
	14:45	10.66	
26/05/97	15:35	7.67	10.88
	16:02	11.31	
	16:33	13.66	
27/05/97	15:33	11.04	11.25
	15:53	10.22	
	16:16	12.48	
27/05/97	10:58	5.97	5.86
	11:17	7.06	
	11:30	4.56	
29/05/97	15:08	10.02	8.94
	15:25	7.47	
	15:37	10.05	
	15:55	8.24	
30/05/97	15:23	5.60	5.90
	15:38	4.20	
	16:00	7.06	
	16:19	6.75	
01/06/97	15:38	6.66	7.25
	15:55	7.72	
	16:12	7.37	
02/06/97	16:14	3.55	5.41
	16:27	5.84	
	16:40	7.21	
	16:51	5.00	
03/06/97	16:27	4.94	5.46
	16:40	5.97	
04/06/97	16:50	24.64	24.64
05/06/97	16:01	25.95	25.95
06/06/97	16:22	6.91	7.43
	16:41	7.94	
07/06/97	14:49	5.73	5.84
	15:02	6.57	
	15:26	5.23	
10/06/97	15:52	9.75	9.75
11/06/97	10:23	12.00	9.71
	10:37	14.41	
	10:57	8.68	
	11:12	12.63	
	15:53	9.76	
	16.11	9.75	
	16:25	3.26	
	16:37	7.26	
12/06/97	15:30	4.03	4.20
	16:25	4.38	
14/06/97	10.03	5.49	5.12
	10.20	6.12	
	10:37	4.99	
	10:54	4.81	
	15:48	6.00	
	16:00	4.26	
	16:13	3.99	
	16:30	5.23	
15/06/97	15:24	6.31	7.03
	15:43	6.69	
	16:01	8.29	
	16:22	8.08	
16/06/97	Time not	2.45	
	recorded	6.70	
		5.03	
17/06/97	16:10	5.39	5.21
	16:24	5.10	
	16:35	7.29	
	16:50	3.06	
19/06/97	12:00	4.55	7.15
	12:30	9.75	
20/06/97	10:24	12.69	13.54
	10:41	16.18	
	10:59	13.07	
	11:17	12.26	
21/06/97	16:00	8.34	10.66
	16:26	12.96	
22/06/97	16:26	5.07	5.07
23/06/97	15:46	15.83	13.39
	16:22	13.77	
	16:39	11.17	
24/06/97	10:11	17.65	22.37
	10:27	15.01	
	15:07	21.22	
	15:34	25.39	
	15:53	28.98	
	16:10	26.00	

eruptions. At Santiaguito, Guatemala, the magma supply rate, required to support the SO_2 emission, was found to be at least four times higher than the observed extrusion rate. This phenomenon of “excess sulfur” has also been documented at SHV (Young et al., 1998a,b), Redoubt (Gerlach et al., 1993) and Unzen (Hirabayashi et al., 1995), as well as for large magnitude eruptions such as El Chichon 1982 and Pintaubo 1991, and has been recently investigated by Kress (1997) and Keppler (1999). During the 1980–1982 Mt. St. Helens eruption, short-term (days–weeks) variations in gas emission rates were interpreted as reflections of shallow intrusion of magma and/or changes in permeability of the dome and conduit lava. Abrupt reduction in SO_2 emission

rates at Mt. St. Helens was interpreted as the result of sealing of the system, whereas long-term exponential emission rate reduction in 1981 and 1982 was believed to result from degassing from a single batch of magma (Casadevall et al., 1983).

Contemporaneous geophysical data, such as ground deformation and seismicity, may indicate pressure changes in the internal system. At Mt. St. Helens, ground deformation increased with SO_2 emission rate during late May and June 1980 (Casadevall et al., 1981). Similar relationships were also observed there from 1984 to 1988 (McGee and Sutton, 1994) when COSPEC SO_2 fluxes and in-situ reducing gas sensors recorded increasing gas emission rates in conjunction with increases in radial tilt and seismicity. During the September 1984 dome building event, increases in SO_2 emission rate and seismicity were observed to precede ground deformation.

At Galeras Volcano, Colombia, long period seismicity data were used in conjunction with COSPEC SO_2 data to interpret the movement of gases from the magma body to the surface, and specifically, the degree of sealing of the system to gas loss (Fischer et al., 1994). Low SO_2 emission rates were typically associated with increased long-period seismicity.

At SHV, enhanced long-period seismicity have not coincided with higher SO_2 emission rates (Young et al., 1998b), even though gas movement in the upper parts of the system has been postulated to have been the cause of seismicity (Neuberg et al., 1998). SO_2 emission rates between 21 July 1995 and 25 June 1997 increased from <2.5 to >6 kg s^{-1} with enhanced emission rates associated with periods of increased magma extrusion rates and pyroclastic activity (Young et al., 1998b). The SO_2 emission rate on 24 June 1997 (30.0 kg s^{-1}), 20 h before the dome collapse event, was the highest ever recorded at SHV, up to that time.

3. Methodology

The application of COSPEC at SHV has been previously reported (Young et al., 1998a) and is thus only summarised here. Observations were obtained along pre-determined road traverses (Fig. 1) with the spectrometer's telescope directed vertically upwards. The spectrometer measures the column mass of SO_2 (in ppm.m) as an attenuation of diffuse-sky radiation in a selected ultraviolet SO_2 absorption feature. The column mass of SO_2 is integrated with respect to the plume width to produce a plume cross-section. This is subsequently multiplied by the wind speed to yield SO_2 emission rates (flux) typically reported in units of kg s^{-1} or t d^{-1} (Millan et al., 1976; Casadevall and Greenland, 1981; Stoiber et al., 1983).

Young et al. (1998a) estimated the absolute accuracy of an individual COSPEC measurement at SHV to be ca. 30%, which is typical of COSPEC errors (McGee, 1992; Bluth et al., 1994). As in most other cases, the wind speed contributes the largest proportion of the total error, because it is measured before and after (rather than during) a set of traverses at the highest accessible point, which was significantly lower (ca. 500 m) than the altitude of the plume and only $\sim$2 m above the ground. Hence, due to the positive wind speed–altitude gradient, COSPEC measurements should be considered a minimum value for SO_2 emission rate (Zapata et al., 1997).

Each individual traverse took 12–20 min depending on the plume azimuth and width, and a set of four traverses and wind speed measurements took up to two hours. COSPEC measurements were attempted on a daily basis and accomplished on 26 of the 32 days between 24 May and 24 June (Table 1). Measurement was impossible during unfavourable meteorological conditions, such as the northerly wind direction, and, more commonly, low light levels caused by haze or cloud. Even during ideal conditions eight traverses a day (including four wind speed measurements) was a realistic maximum. Data obviously could not be obtained at night or around noon when direct sunlight could have damaged the instrument's photomultiplier tube.

The seismic (Aspinall et al., 1998; Miller et al., 1998) and the tiltmeter networks (Voight et al., 1998) have been reviewed previously and data for the period of interest discussed. Details of the location and orientation of both networks are given in Fig. 1. The seismic signal was classified into seven event classes (Miller et al., 1998) and reported as 10 min averages of real-time seismic amplitude measurement (RSAM, Endo and Murray, 1991). The event classes include volcano-tectonic (VT) earthquakes (>5 Hz), long period (LP) earthquakes (1–2.5 Hz) and hybrid earthquakes (0.5–4 Hz) which have a mix of characteristics between VT and LP events.

The data from the seismic network were received in real time and the tilt data where received at eight minute intervals, with transmission taking less than 10 s. The difference in temporal resolution of the three different data types presents the greatest problem in integration and analysis. Whilst the tilt and seismic data can be considered continuous, the COSPEC emission rate measurements provide snapshots at irregular intervals. For the data to be compared directly, similar sampling intervals are desirable, but this is not possible given the nature of the COSPEC measurement technique. Instead, the tilt data were reduced to tilt cycle amplitude and the hybrid count to earthquakes per hour. This provided a similar sampling interval for the period of interest (26 mean COSPEC measurements and 44 tilt cycle amplitudes, with hybrids during 10 cycles) which facilitated direct comparison of the datasets and investigation of degassing during an individual tilt cycle.

To investigate systematic variation in degassing during an individual tilt cycle, the COSPEC data were described according to their timing relative to the start and end of a tilt cycle (Fig. 2). As the tilt cycles were not symmetrical, each tilt cycle was divided into inflation and deflation sections by the position of the inflation peak. Given that at least parts of the COSPEC dataset correlate with the tilt cycle amplitude, further re-working was required to remove that bias; it is possible every pre-maximum measurement was taken during periods of lower deformation, implying lower emission rate during inflation. To correct for this the COSPEC data were normalised with respect to the tilt cycle amplitude by multiplying by the ratio between the individual tilt amplitude and the maximum tilt amplitude (26.32 μrad).

4. Results

The COSPEC record reported begins on 24 May 1997 after a lapse of nearly 2 months while the spectrometer was fixed off-island. For the first 5 days, the tilt cycle was well developed with amplitudes between 18 and 25 μrad associated with peak hybrid occurrences of 15–20 hybrids per hour (Fig. 3). Larger tilt cycle amplitudes coincided with bursts of hybrid seismicity and raised SO_2 emission rates. Increases in tilt cycle amplitude to >10 μrad, RSAM peaks of >200 (discounting pyroclastic flow spikes) and increasing SO_2 emission rates of $>11.5\ kg\ s^{-1}$ all occurred with increasing hybrid activity. The intermediate period from 2 to 21 June is characterised by lower tilt cycle amplitudes and lower gas fluxes, except during 4th and 5th June when pyroclastic flows reached the sea on the eastern side of the island. This caused significant increases in SO_2 emission rates (to $>13\ kg\ s^{-1}$) and an RSAM spike but interestingly little or no change in the tilt cycle amplitude.

During the whole observation period, there is a broad correlation between SO_2 emission rate, tilt cycle amplitude and peak hybrid earthquake occurrence (Fig. 4). Higher SO_2 fluxes are associated with larger tilt amplitude and an increase in the number of hybrid earthquakes per cycle inside. The spike in SO_2 on June 4–5 reflects pyroclastic flow generation. A VT earthquake swarm on 22 June (Voight et al., 1998), possibly caused by an increase in magma pressurisation or the passage of more gas-rich magma (Miller et al., 1998), preceded the resurgence of hybrid seismicity by a few hours. The re-occurrence of enhanced hybrid seismicity coincided exactly with an increase in tilt cycle amplitude and heightened SO_2 emission rates.

We further investigate the correlation between the tilt cycle amplitude and SO_2 emission rate in two ways: (1) by examining different sub-periods; (2) by looking for improved correlation above a certain tilt amplitude threshold. Figs. 3 and 4 suggest that the correlation improves during certain times of the period of interest, so the data have been divided into arbitrary periods based on the tilt cycle amplitude, hybrid seismicity and SO_2 emission rate trends. Period 1 is characterised by decreasing tilt cycle amplitude, SO_2 emission rate and hybrid seismicity, Period 2 by raised SO_2 associated with pyroclastic flows, Period 3 by low SO_2 degassing, seismicity and tilt, and Period 4 by increasing tilt, SO_2 output and hybrid earthquake occurrences. Correlation coefficients have been calculated for the data (Fig. 5a) from 24 May to 3 June (Period 1) and from 22–24 June (Period 4), which indicates that for periods of raised hybrid seismicity the correlation is stronger.

Stronger correlations are also observed for periods of high tilt amplitude (>12 μrad, (Fig. 5b). The overall correlation for the data series is 0.14 but

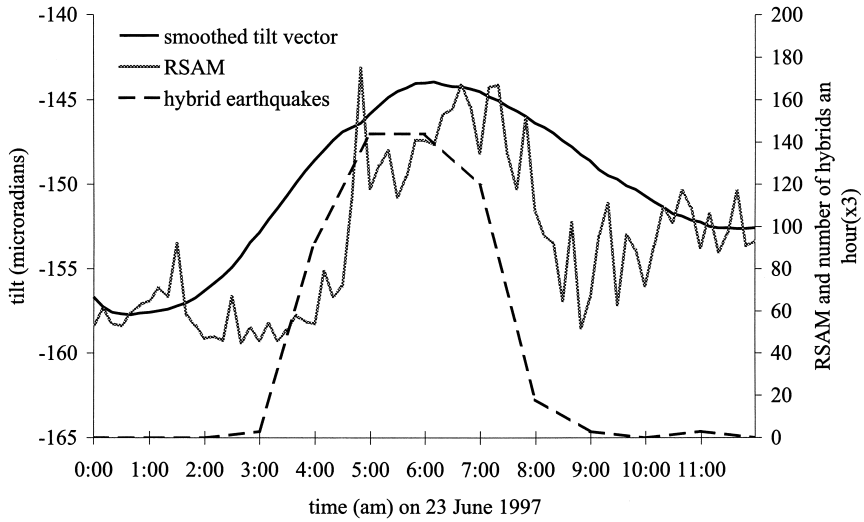

Fig. 2. Diagram showing relative timing of tilt cycle deformation, 10 min RSAM average and number of hybrid earthquakes an hour for one tilt cycle during the morning of 23 June 1997.

above 12 μrad the correlation improved to 0.73. Again, this suggests that as the cycles become more developed and hybrid seismicity increases the correlation between degassing and deformation improves.

For Period 1, when the tilt amplitude was showing a general decreasing trend, any systematic variation is unclear (Fig. 6). It appears that some degassing occurs during hybrid activity and inflation (0.2–0.5 tilt cycles) and during deflation. The highest normalised COSPEC values are coincident with the inflation maxima (defined 0.52, the average peak position) and during deflation at 0.7–0.8 tilt cycles. For Period 4, when tilt cycle amplitude, hybrid activity and SO_2 emission rate were increasing, a similar pattern is observed with a peak during deflation at 0.7–0.8 tilt cycles. High, normalised emission rates are also a feature of the inflation part of the tilt cycle for Period 4 during the hybrid earthquake swarms.

5. Discussion

Several processes can influence SO_2 emission rates over a deformation cycle, including: (1) release of gas from the conduit to the atmosphere via cracks in the conduit wall or dome; (2) entrapment, or flow-retardation, of gas in the free-space (pores and fractures) in the dome, released during partial dome disruption; (3) direct release of gas from freshly extruded magma to the atmosphere; and (4) release of gas in explosive eruptions from magma fragmentation (this process is not important for the period discussed here). In addition, process (2) can be subdivided into: (2a) dome cracking and disruption by magma extrusion; (2b) dome disruption by generation of rock falls and pyroclastic flows, in which a component of gas release may occur from the pyroclastic deposits for some time after the initial disruption (Young et al., 1998a,b).

These processes could result in variable SO_2 emission during a deformation cycle. In process (1) degassing can occur at all times but, for well-developed cycles, gas emission rate would increase during the pressure build up, toward peak inflation, when gas flow gradients are greatest. Some delayed gas release can occur in process (2), but most gas released in this process would occur as the dome is broken up soon after peak inflation, by extruding magma possibly accompanied by partial dome collapse with rockfalls or pyroclastic flows. Likewise, the processes (3) and (4) would increase emission rate soon after peak inflation, with a transient decay in gas flux associated with degassing lava or pyroclastic deposits.

Several models have been proposed for the generation of cyclicity at silicic volcanoes. These

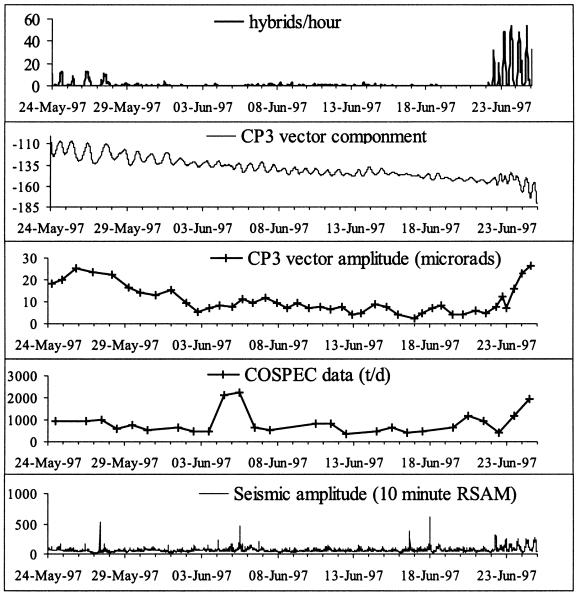

Fig. 3. Raw tiltmeter (CP3 vector), COSPEC emission rates, 10 min RSAM, number of hybrids per hour and tilt cycle vector amplitude for the period 24 May 1997–24 June 1997.

include periodic, unstable retardation of magma flow due to increased viscosity from shallow degassing and microlite crystallisation (Sparks et al., 1997; Voight et al., 1998, 1999; Wylie et al., 1999) and compression of Newtonian fluids by a constant supply rate combined with a particular stick–slip boundary condition (Denlinger and Hoblitt, 1999). An important parameter for these models is the pressure exerted on the rising magma and the generation of large excess pressures. The causes of pressurisation differ from model to model. In the models of Sparks (1997) and Voight et al. (1998, 1999), pressurisation is influenced by vertical viscosity gradients induced by degassing and microlite crystallisation, whereas in the Denlinger and Hoblitt (1999) model pressurisation is affected by unstable flow rates caused by boundary condition interactions. These differences have ramifications on the timing of maximum degassing with a tilt cycle. None of the models preclude shallow degassing on ascent into the atmosphere through fracture and cracks (degassing process 1) but all imply that degassing would peak in systematic relation to, but out of phase with, peak inflation. The relation between the rate of degassing and peak inflation is clarified by the model of Wylie et al. (1999), which quantifies the mechanism of Voight et al. (1999). Wylie et al. (Fig. 3) show that the peak rate of magma flow and mean dissolved volatiles in the upper conduit are out of phase with peak inflation and the pressure peak. Thus the peak flow rate of volatile charged magma is predicted to occur during the deflation phase of the tilt cycle, as qualitatively suggested by Fig. 6.

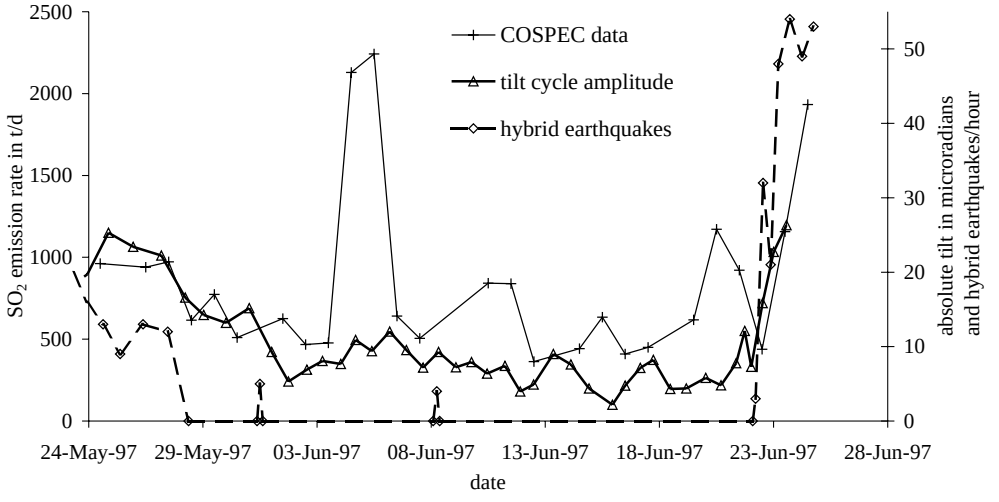

Fig. 4. The relationship between the COSPEC SO_2 emission rate data, the CP3 tilt cycle vector amplitude and the number of hybrids per hour. Note the dramatic increase in all three parameters on the 22 June 1997.

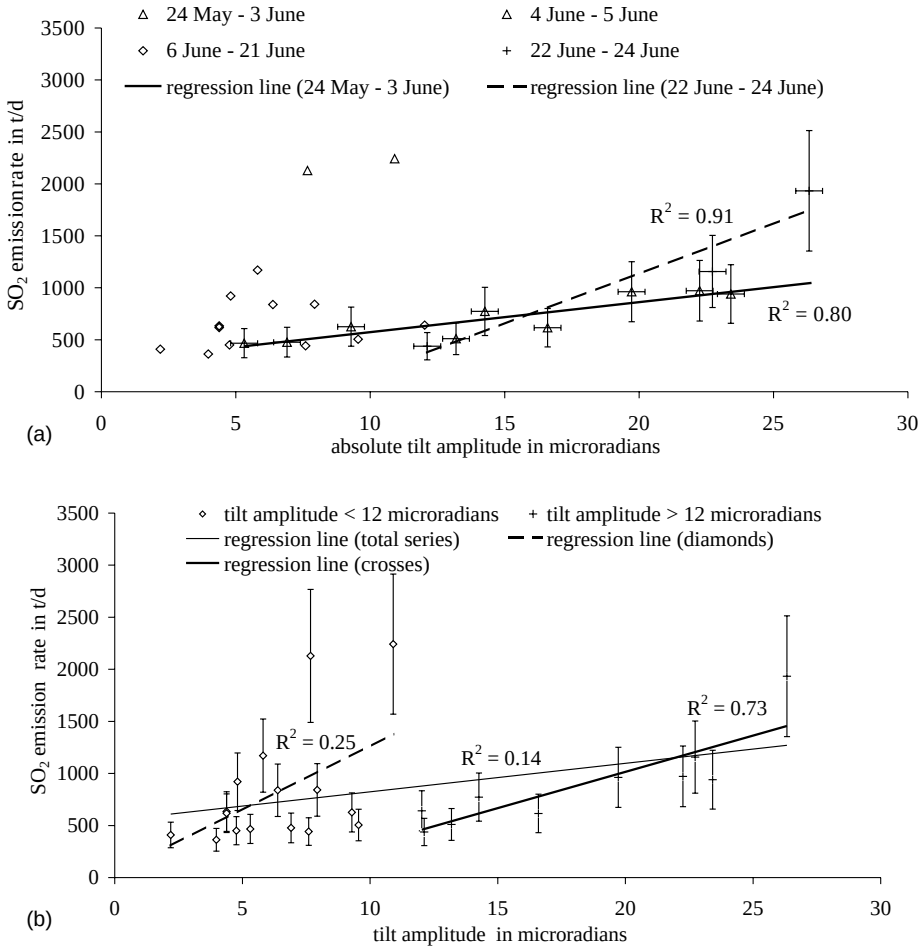

Fig. 5. (a) Correlation between tilt cycle amplitude and SO_2 emission rate based on using different periods of the month prior to the 25 June collapse. (b) Correlation between tilt cycle amplitude and SO_2 emission rate based on using a procedure to calculate whether the correlation significantly improves above a certain threshold (in tilt cycle amplitude).

From Fig. 6, it is clear that in the immediate build up to the 25 June dome collapse there was significant degassing (>20 kg s^{-1}) during the hybrid swarm that took place between 1400 and 2100 hours on 24 June. Hybrid seismicity plays a key role during the build-up of pressure in the conduit prior to extrusion and has been interpreted at SHV in two ways, which may relate directly to either the degassing (Sparks/Voight) or stick–slip (Denlinger and Hoblitt) models. Either the hybrids are caused by violent degassing into adjacent cracks (White et al., 1998), or as stick–slip motion of magma sliding against the conduit wall. However, the mechanism is compatible with the Voight et al. (1998, 1999) model, in which hybrids are interpreted to be caused by pressure build-up. Both of the hybrid/degassing models are consistent with the SO_2 emission rate data pertaining to systematic variation during a tilt cycle.

The VT swarm on the 22 June 1997, which preceded the resumption of hybrid earthquake swarms, may signify the passage of more gas-rich, buoyant magma, or an increase in flow rate (Miller et al., 1998) towards the surface, or both. The swarms of hybrid earthquakes that followed the VT swarm

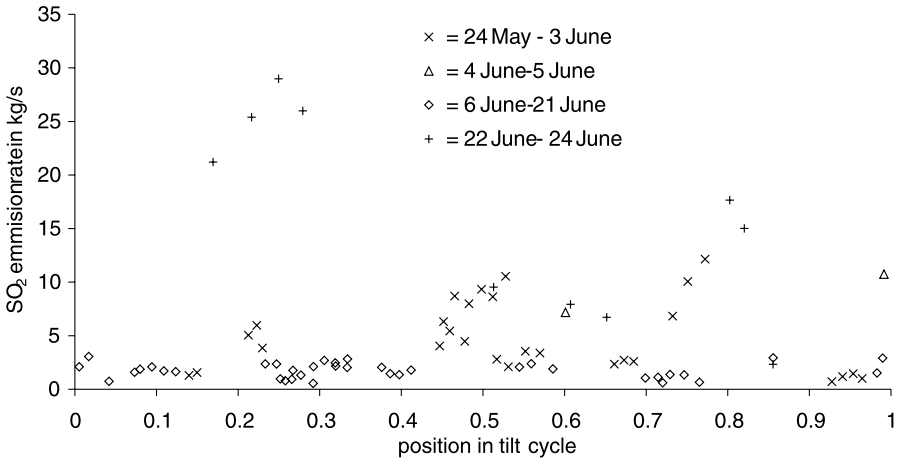

Fig. 6. Diagram showing possible variation of SO_2 emission rate during and individual tilt cycle for different periods of interest. The cycle begins and ends at tilt minima; peak inflation is ~ 0.5.

correlated well with the increases in tilt cycle amplitude and SO_2 emission rate that preceded the 25 June dome collapse. Superimposed on this increasing trend is a systematic variation of emission rate within an individual tilt cycle, as previously discussed.

6. Conclusions

SO_2 emission rates measured by COSPEC have been correlated with tiltmeter ground deformation data, which has previously been strongly correlated with seismicity, particularly hybrid earthquake swarms (Miller et al., 1998). During periods of regular hybrid swarms, SO_2 emission rate correlated strongly with ground deformation ($r^2 = 0.73–0.91$). During the four days prior to the 25 June dome collapse, SO_2 emission rate, tilt cycle amplitude and peak hybrid occurrence per cycle, all increased. This observation is consistent with the rise of more gas-rich magma or an increase in flow rate (or both) and subsequent increases in pressure which may have caused the hybrid seismicity. Some systematic variation in SO_2 emission across an individual tilt cycle is observed, although the poor accuracy of COSPEC measurements, and random time of measurements clouds interpretation. However, the data seem consistent with the model of Wylie et al. (1999), which accounts for a phase shift of flow rate with respect to peak pressure.

Acknowledgements

The authors gratefully acknowledge the MVO, BGS and NERC for supporting the COSPEC measurement campaign and NERC for studentship (under grant number GT4/96/60/EO). BV also acknowledges the support of NSF. We would particularly like to thank Bill Rose and an anonymous referee for thorough reviews, which have greatly improved the paper.

References

Aspinall, W.P., Miller, A.D., Lynch, L.L., Latchman, J.L., Stewart, R.C., White, R.A., Power, J.A., 1998. Soufrière Hills eruption, Montserrat, –: Volcanic earthquake locations and fault plane solutions. Geophys. Res. Lett. 25 (18), 3397–3401.

Bluth, G.J.S., Casadevall, T.J., Schnetzler, C.C., Doiron, S.D., Walter, L.S., Krueger, A.J., Badruddin, M., 1994. Evaluation of SO_2 emissions from explosive volcanism: the 1982–1983 eruptions of Galunggung, Java, Indonesia. J. Volcanol. Geotherm. Res. 63, 243–256.

Casedevall, T.J., Greenland, L.P., 1981. SO_2 emission rates at Mt. St. Helens from March 29 through December 1980. In: Lipman, Mullineaux (Eds.), The 1980 Eruption of Mt. St. Helens, Washington. USGS, Prof. Pap. No. 1250. pp. 193–207.

Casadevall, T.J., Johnston, D.A., Harris, D.M., Rose, W.I., Malinconico, L.L., Stoiber, R.E., Bornhorst, T.J., Williams, S.N., Woodruff, L., Thompson, J.M., 1981. The chemistry of gases emanating from Mt. St. Helens, May–September 1980. In: Lipman, Mullineaux (Eds.), The 1980 Eruption of Mt. St. Helens, Washington. USGS, Prof. Pap No. 1250. pp. 221–226.

Casadevall, T.J., Rose, W.I., Gerlach, T.M., Greenland, J., Wunderman, E., Symonds, R., 1983. Gas emissions and the eruptions of Mt. St. Helens. Science 221, 1283–1385.

Denlinger, R.P., Hoblitt, R.P., 1999. Cyclic eruptive behaviour of silicic volcanoes. Geology 27 (5), 459–462.

Endo, E.T., Murray, T., 1991. Real-time Seismic Amplitude Measurement (RSAM)—a volcano monitoring and prediction tool. Bull. Volcanol. 53 (57), 533–545.

Fischer, T.P., Morrisey, M.M., Clavache, M.L., Gomez, D., Torres, R., Stix, J., Williams, S.N., 1994. Correlations between SO_2 flux and long-period seismicity at Galeras volcano. Nature 368, 135–137.

Gerlach, T.M., Westrich, H.R., Casadevall, T.J., Finnegan, D.L., 1993. Vapor saturation and accumulation in magmas of the 1989–1990 eruption of Redoubt volcano, Alaska. J. Volcanol. Geotherm. Res. 62, 317–337.

Hirabayashi, J., Ohba, T., Nogami, K., Yoshida, M., 1995. Discharge rate of SO_2 from Unzen Volcano, Kyushu, Japan. Geophys. Res. Lett. 22, 1709–1712.

Keppler, H., 1999. Experimental evidence for the source of excess sulfur in explosive volcanic eruptions. Science 284, 1652–1654.

Kress, V., 1997. Magma mixing as a source for Pinatubo sulphur. Nature 389, 591–593.

McGee, K.A., 1992. The structure, dynamics and chemical composition of non-eruptive plumes from Mt. St. Helens, 1980–88. J. Volcanol. Geotherm. Res. 51, 269–282.

McGee, K.A., Sutton, J., 1994. Eruptive activity at Mt. St. Helens Washington, USA, 1984–1988: a gas geochemistry perspective. Bull. Volcanol. 56, 435–446.

Millan, M., Gallant, A.J., Turner, H.E., 1976. The application of correlation spectroscopy to the study of dispersion from tall stacks. Atmos. Env. 10, 499–511.

Miller, A.D., Stewart, R.C., White, R.A., Luckett, R., Baptie, B.J., Aspinall, W.P., Latchmann, J.L., Lynch, L.L., Voight, B., 1998. Seismicity associated with dome growth and collapse at the Soufriere Hills Volcano, Montserrat. Geophys. Res. Lett. 25 (18), 3401–3404.

Neuberg, J., Baptie, B., Luckett, R., Stewart, R., 1998. Results from the broadband seismic network. Geophys. Res. Lett. 25 (19), 3661–3664.

Sparks, R.S.J., 1997. Causes and consequences of pressurisation in lava dome eruptions. Earth Planet. Sci. Lett. 150, 177–189.

Stoiber, R.E., Malinconico, L.L., Williams, S.N., 1983. Use of the correlation spectrometer at volcanoes. In: Tazieff, Sabroux (Eds.). Forecasting Volcanic Events. Elsevier, Amsterdam, pp. 425–444.

Voight, B., Hoblitt, R.P., Clarke, A.B., Lockhart, A.B., Miller, A.D., Lynch, L., McMahon, J., 1998. Remarkable cyclic ground deformation monitored in real time on Montserrat and its use in eruption forecasting. Geophys. Res. Lett. 25 (18), 3405–3409.

Voight, B.V., Sparks, R.S.J., Miller, A.D., Stewart, R.C., Hoblitt, R.P., Clarke, A.B., Ewart, J., Aspinall, W., Baptie, B., Druit, T.H., Herd, R., Jackson, P., Lockhart, A.B., Loughlin, S.C., Luckett, R., Lynch, L., McMahon, J., Norton, G.E., Robertson, R., Watson, I.M., Young, S.R., 1999. Magma flow instability and cyclic activity at Soufriere Hills Volcano, Montserrat B.W.I. Science 283, 1138–1142.

White, R.A., Miller, A.D., Lynch, L., Power, J., 1998. Observations of the hybrid seismicity at Soufriere Hills Volcano Montserrat: July to September. Geophys. Res. Lett. 25 (19), 3657–3660.

Wylie, J.J., Voight, B., Whitehead, J.A., 1999. Instability of magma flow from volatile-dependent viscosity. Science 283, 1883–1885.

Young, S., Sparks, S., Robertson, R., Lynch, L., Aspinall, W., 1997. Eruption of Soufriere Hills Volcano in Montserrat continues. EOS Trans. AGU 78, 404–409.

Young, S.R., Sparks, R.S.J., Aspinall, W.P., Lynch, L.L., Miler, A.D., Robertson, R.E.A., Shepherd, J.B., 1998. Overview of the eruption of Soufriere Hills Volcano, Montserrat, 18 July to December . Geophys. Res. Lett. 25 (18), 3389–3392.

Young, S.R., Francis, P.W., Barclay, J., Casadevall, T.J., Gardner, C.A., Darroux, B., Davies, M.A., Delmelle, P., Norton, G.E., Maciejewski, A.J.H., Oppenheimer, C.M.M., Stix, J., Watson, I.M., 1998. Monitoring SO_2 emissions at the Soufriere Hills Volcano: implications for changes in eruptive conditions. Geophys. Res. Lett. 25 (19), 3681–3684.

Zapata, J.A.G., Calvache, M.L.V., Cortes, G.P.J., Fischer, P.F., Garzon, G.V., Gomez, D.M., Narvaez, L.M., Ordonez, M.V., Ortega, A.E., Stix, J., Torres, R.C., Williams, S.N., 1997. SO_2 fluxes from Galeras Volcano, Columbia, 1989–1995. J. Volcanol. Geotherm. Res. 77, 195–208.